MANIPULATION

MOGrip: Gripper for multiobject grasping in pick-and-place tasks using translational movements of fingers

Jaemin Eom[1], Sung Yol Yu[1], Woongbae Kim[2,3], Chunghoon Park[1,4], Kristine Yoonseo Lee[1], Kyu-Jin Cho[1]*

Humans use their dexterous fingers and adaptable palm in various multiobject grasping strategies to efficiently move multiple objects together in various situations. Advanced manipulation skills, such as finger-to-palm translation and palm-to-finger translation, enhance the dexterity in multiobject grasping. These translational movements allow the fingers to transfer the grasped objects to the palm for storage, enabling the fingers to freely perform various pick-and-place tasks while the palm stores multiple objects. However, conventional grippers, although able to handle multiple objects simultaneously, lack this integrated functionality, which combines the palm's storage with the fingers' precise placement. Here, we introduce a gripper for multiobject grasping that applies translational movements of fingertips to leverage the synergistic use of fingers and the palm for enhanced pick-and-place functionality. The proposed gripper consists of four fingers and an adaptive conveyor palm. The fingers sequentially grasp and transfer objects to the palm, where the objects are stored simultaneously, allowing the gripper to move multiple objects at once. Furthermore, by reversing this process, the fingers retrieve the stored objects and place them one by one in the desired position and orientation. A finger design for simple object translating and a palm design for simultaneous object storing were proposed and validated. In addition, the time efficiency and pick-and-place capabilities of the developed gripper were demonstrated. Our work shows the potential of finger translation to enhance functionality and broaden the applicability of multiobject grasping.

INTRODUCTION

Humans efficiently move multiple objects by grasping and transferring them together. These grasping strategies, named multiobject grasping, decrease the entire pick-and-place process time by reducing the repetitive motion of the arm. Humans perform diverse multiobject grasping strategies depending on the task and environment, exploiting their dexterous hand skills, such as pinch grasp, palmar grasp, and other advanced manipulation skills; these include pinching objects between a pair of fingers or enveloping multiple objects using the palm and fingers (*1*). Advanced manipulation skills enhance the versatility of multiobject grasping by enabling humans to perform more complex manipulation tasks. Specifically, finger-to-palm translation allows the pinched objects to be transferred by the fingertips into the palm for stable storage (Fig. 1A) (*2*, *3*). This process frees the fingertips to grasp new targets and can be repeated to simultaneously store multiple objects in the palm (*4*, *5*). Furthermore, after moving the objects, humans use palm-to-finger translation to transfer objects stored in the palm to the fingertips one by one. This translation process enables the fingertips to retrieve the objects and perform diverse placement tasks, such as shelving or hanging objects in desired orientations. In summary, using the translational movements of fingertips in multiobject grasping leverages the strength of both the fingers and the palm, maintaining the fingers' degrees of freedom while storing multiple objects. This synergistic approach of the human hand offers a more versatile multiobject pick-and-place capability compared with other multiobject grasping methods, while it retains the efficiency from moving multiple objects together.

Inspired by the functions of the human hand, various robotic grippers have been developed by selectively adopting specific hand capabilities instead of replicating the entire hand's functionalities. Most gripper research focuses on analyzing key principles of specific hand functions and integrating these insights into their design. For example, underactuated grippers use differential mechanisms to achieve force closure, similar to human hands, enabling effective grasping of objects of diverse shapes (*6*–*8*). Additionally, some grippers use a regrasping process to change the orientation of objects for precise placement (*9*, *10*). These grippers incorporate vision and tactile sensing, essential elements in human regrasping techniques. Robotic grippers for multiobject grasping have also emerged as potential solutions for improving productivity by applying the human strategy of moving multiple objects at once. However, previous studies primarily focused on effectively grasping multiple items simultaneously, using a palmar grasp with either a fingered gripper (*11*–*13*) or a parallel gripper (*14*–*19*) or using other grasping methods (*20*–*27*). These approaches, although suitable for object transportation, face challenges in precisely placing each object in the desired position and orientation. This difficulty arises because the grasped objects interfere with the placement of other objects, or they are placed in a group. Therefore, as conventional grippers have advanced, there is a growing necessity for studies on grippers designed for multiobject grasping that not only effectively grasp and transfer multiple items together but also accurately place them. A fundamental principle in human manipulation for this capability is the synergistic use of the palm's storage capacity and the fingers' placing ability, enabled by the translational movements of the fingers. Therefore, further exploration into grippers that leverage the translation of fingers is essential for multiobject grasping in diverse situations.

[1]Biorobotics Laboratory, Soft Robotics Research Center, Institute of Advanced Machines and Design, Department of Mechanical Engineering, Institute of Engineering, Seoul National University, Seoul 08826, Republic of Korea. [2]Artificial Intelligence and Robotics Institute, Korea Institute of Science and Technology (KIST), Seoul 02792, Republic of Korea. [3]Korea Institute of Science and Technology Europe (KIST-EUROPE), 66123 Saarbrücken, Germany. [4]Manufacturing Core Technology Team, Global Technology Research, Samsung Electronics Co. Ltd., Gyeonggi-do 16677, Republic of Korea.
*Corresponding author. Email: kjcho@snu.ac.kr

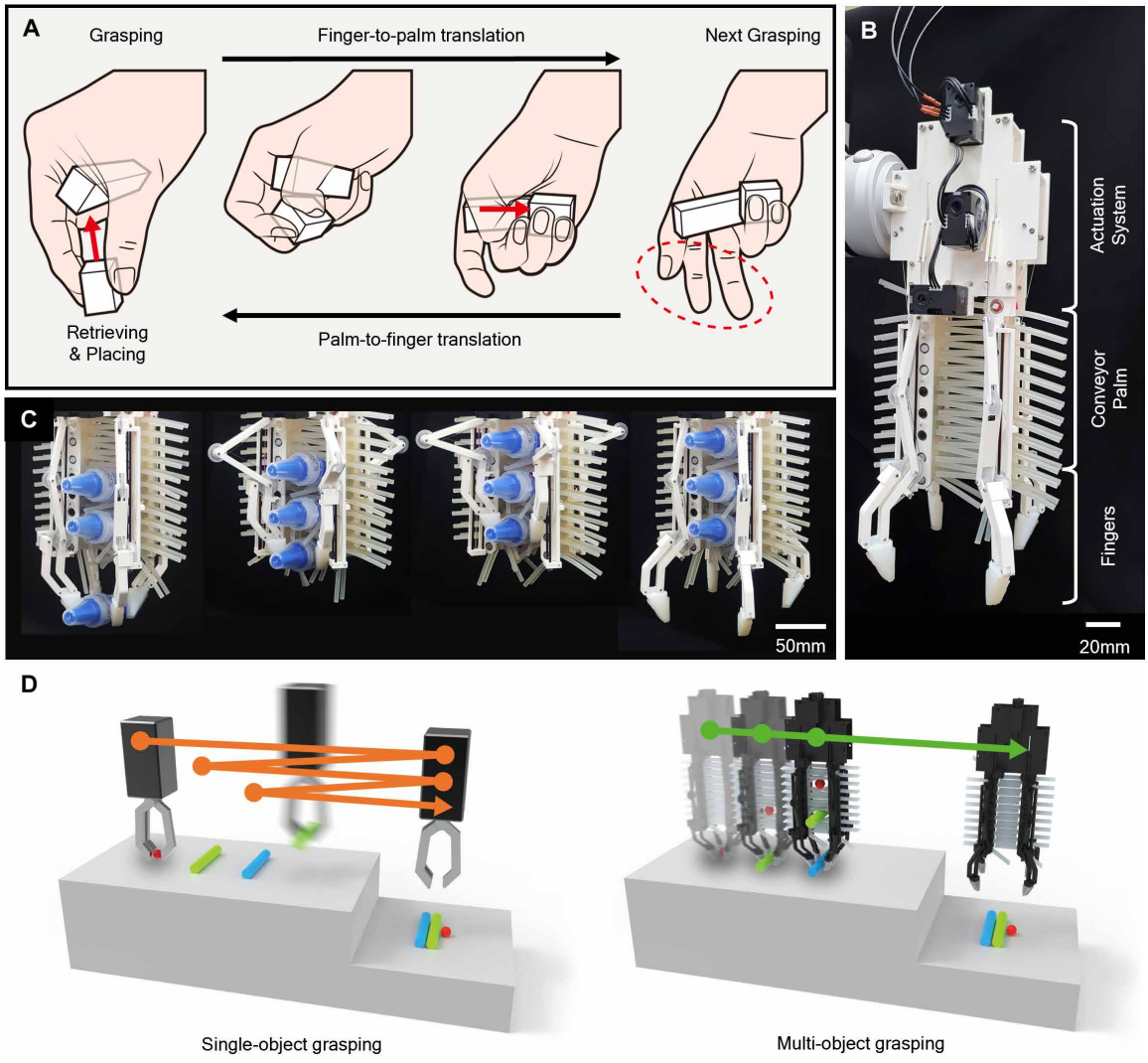

Fig. 1. The multiobject gripper inspired by humans' multiobject grasping using translational movements of fingertips. (**A**) The sequence of a human multiobject grasping method using the translational movement of the fingers allows for synergistic use of the fingers and palm. (**B**) Proposed multiobject gripper. It consists of four fingers, a conveyor palm, and an actuation system including three motors. (**C**) The concept of the proposed multiobject gripper corresponds to the human strategy. The proposed gripper uses the translational movement of the fingers to store or retrieve objects for picking and placing each object. (**D**) Comparison of the manipulator's travel distances between single-object grasping and multiobject grasping.

Here, we introduce a robotic gripper for multiobject grasping that applies finger-to-palm and palm-to-finger translation to use the delicate pick-and-place capabilities of fingertips while simultaneously holding multiple objects together in the palm (Fig. 1B). The developed gripper is capable of not only versatile pick and place of single objects using four fingertips but also simultaneous storage of multiple objects through the palm's enveloping ability. The proposed gripper can pick single objects from various orientations using the underactuated fingers and subsequently transfer them to the palm through finger-to-palm translation for storing and moving them together (Fig. 1C). After moving the objects, the gripper retrieves the stored objects individually with the fingertips through palm-to-finger translation for precise object placement. By applying the proposed grasping method, the developed gripper can successfully reduce the travel distance of the manipulator during the pick-and-place process compared with that of single-object grippers (Fig. 1D).

To simplify the delicate translational movements of fingertips and grasping performed by humans, we applied a decoupling linkage to the fingers for mechanically separating the grasping and translation motions. Furthermore, to facilitate a simple storing process and to increase the storing capacity compared with a human palm, we proposed an adaptive conveyor palm composed of a pair of opposing belts with elastic hairs arranged on their surfaces. When the belts rotate, objects are inserted between the hairs, enabling the simultaneous storage and transfer of multiple objects. With these design methods, the proposed gripper performs grasping, translating, storing, and retrieving the objects with only three motors. To validate the proposed gripper, the process times of multiobject grasping and single-object grasping were compared in a laboratory-scale logistics environment, and the gripper's pick-and-place capabilities were also demonstrated. Through a mechanical design that simplifies finger translation and the implementation of the conveyor palm, we have

proposed a unique grasping approach that leverages the pick-and-place capabilities of fingers and the simultaneous storing ability of the palm, broadening the versatility of multiobject grasping. For simplicity, in this paper, the gripper designed for multiobject grasping is referred to as the "multiobject gripper," and the gripper that picks up and moves objects one at a time is called the "single-object gripper."

RESULTS

Multiobject gripper inspired by humans' sequential multiobject grasping strategies

Inspired by the human multiobject grasping strategy, using translational movements of the fingers, we developed a multiobject gripper that uses fingers capable of finger-to-palm translation and palm-to-finger translation, along with a palm suitable for simultaneous storage. The developed gripper is illustrated in Fig. 2. The proposed gripper consisted of four fingers and a conveyor palm (Fig. 2A). Each of the four fingers was placed on a slider, and they were driven by two tendons called the "grasping tendon" and the "translating tendon" (Fig. 2B). The grasping tendon produces the grasping motion of the finger, and the translating tendon actuates the finger-to-palm translation of the finger. The grasping tendon wrapped around the free-rotating pulleys, centered on the three revolute joints of the decoupling links and attached to the parallelogram linkage finger. The translating tendon was directly connected to a slider. A torsional spring was inserted between the finger and the slider, and a linear spring was embedded between the slider and the linear guide. These passive elements generate a restoring force that returns the finger to its initial state without the need for additional tendons. For the storage, a motor and a gear system were used to rotate the belts with polymer hairs embedded on their surfaces (Fig. 2C). The grasping motion of the four fingers was underactuated by a single motor using a moving pulley system, as introduced in previous research (*28*), to adaptively grasp objects with simplified control (Fig. 2D). The four translating tendons were also driven by a single motor and were connected on the same pulley, allowing the fingers to move an equal distance from each other. By using an appropriate underactuation mechanism suitable for grasping and translating tendons, the number of required motors and the complexity of the system were reduced.

Figure 2E illustrates the multiobject grasping sequence of the developed gripper. When the grasping tendon was pulled, the fingers rotated to grasp an object (Fig. 2E, i and ii). Subsequently, actuating the translating tendon caused the fingers to translate the object into the storage while maintaining the grasp (Fig. 2E, ii and iii). When the object arrived at the entrance of the storage, the belts started to rotate at the same speed as the translational movement of fingers and stored the object between their hairs (Fig. 2E, iii and iv). Finally, once the grasping and translating tendons were released, the fingers returned to their initial position because of the restoring force of the torsional spring and the linear spring. By reversing the aforementioned grasping and storing processes, the gripper could individually retrieve and place objects in the desired orientation.

Compared with the conventional single-object grasping process, the additional translating and storing processes may slow down the overall procedure. Therefore, to enhance the time efficiency of the proposed grasping method, it was necessary to design a simple translating and storing mechanism. Decoupling links simplified the object grasping and translating processes of the fingers, and the conveyor palm with elastomeric hairs enabled the straightforward translation and storage of multiple objects using a single motor.

Finger design for decoupled grasping and translation

Each gripper finger consisted of a revolute joint and a prismatic joint for directly grasping and translating objects. To reduce the inertia of the fingers during the translation process, tendon-driven mechanisms were used instead of directly attaching motors to the joints of the fingers. Figure 3A shows a finger constructed with one of the intuitive RP (revolute and prismatic) joints; the finger was connected to the slider by a revolute joint, and the slider moved linearly along a linear guide. In this design, pulling the grasping tendon not only rotated the finger but also translated the finger. Similarly, pulling the translating tendon loosened the grasping tendon, causing grasping failure of the finger. This problem generally occurs in a multijoint robotic system driven by multiple tendons (*29*). To address this issue, studies for controlling coupled tendons (*30*, *31*) or designing systems that mechanically decouple the kinematics of tendons (*32*–*35*) have been proposed. Especially, tendon decoupling designs enable direct motion control, reducing control costs for each finger. The fundamental principle of the tendon decoupling design is that when the length of one tendon changes, the lengths of other tendons must remain constant. As an example, a constant tendon system was proposed (*35*) to maintain the grasp on an object while a tendon-driven finger translated the object in a direction parallel to the palm.

On the basis of this principle, we proposed a finger design incorporating two decoupling links that can decouple grasping and translation motions, which has not been explored previously. Figure 3B shows the finger made of RP planar linkage with a decoupling linkage. When the finger was pulled toward the palm, the grasping tendon was released at pulley 2 and further wound at pulleys 1 and 3 (Fig. 3C). The amount of winding and unwinding of the grasping tendon can be equalized by choosing appropriate radii of the pulleys and lengths of decoupling links, allowing finger translation without changing the length of the grasping tendon. Therefore, the decoupling linkage maintained the finger's rotation angle during finger translation and prevented grasping failure. In addition, the decoupling linkage can withstand the pulling force of the grasping tendon, preventing translation of the finger when the grasping tendon is pulled (Fig. 3D).

As a result, adding a decoupling linkage to the RP planar linkage created a decoupled movement of the joints, allowing direct control of each joint. The design conditions of the decoupling linkage for separating the kinematics of tendons have been derived as

$$l_1 = l_2, \quad r_2 = \frac{r_1 + r_3}{2} \tag{1}$$

where l_1 and l_2 are lengths of decoupling links and r_1, r_2, and r_3 are the radii of pulleys 1, 2, and 3, respectively (Fig. 3, B and E). A detailed explanation of the design conditions is available in the "Design condition of decoupling linkage" section in Supplementary Methods and fig. S1.

When the decoupling links did not satisfy the given design conditions (Eq. 1), the finger exhibited coupled grasping and translating motion. Pulling the translating tendon altered the grasping angle, whereas actuating the grasping tendon induced translational movement of the finger. To analyze the finger's movement in response to

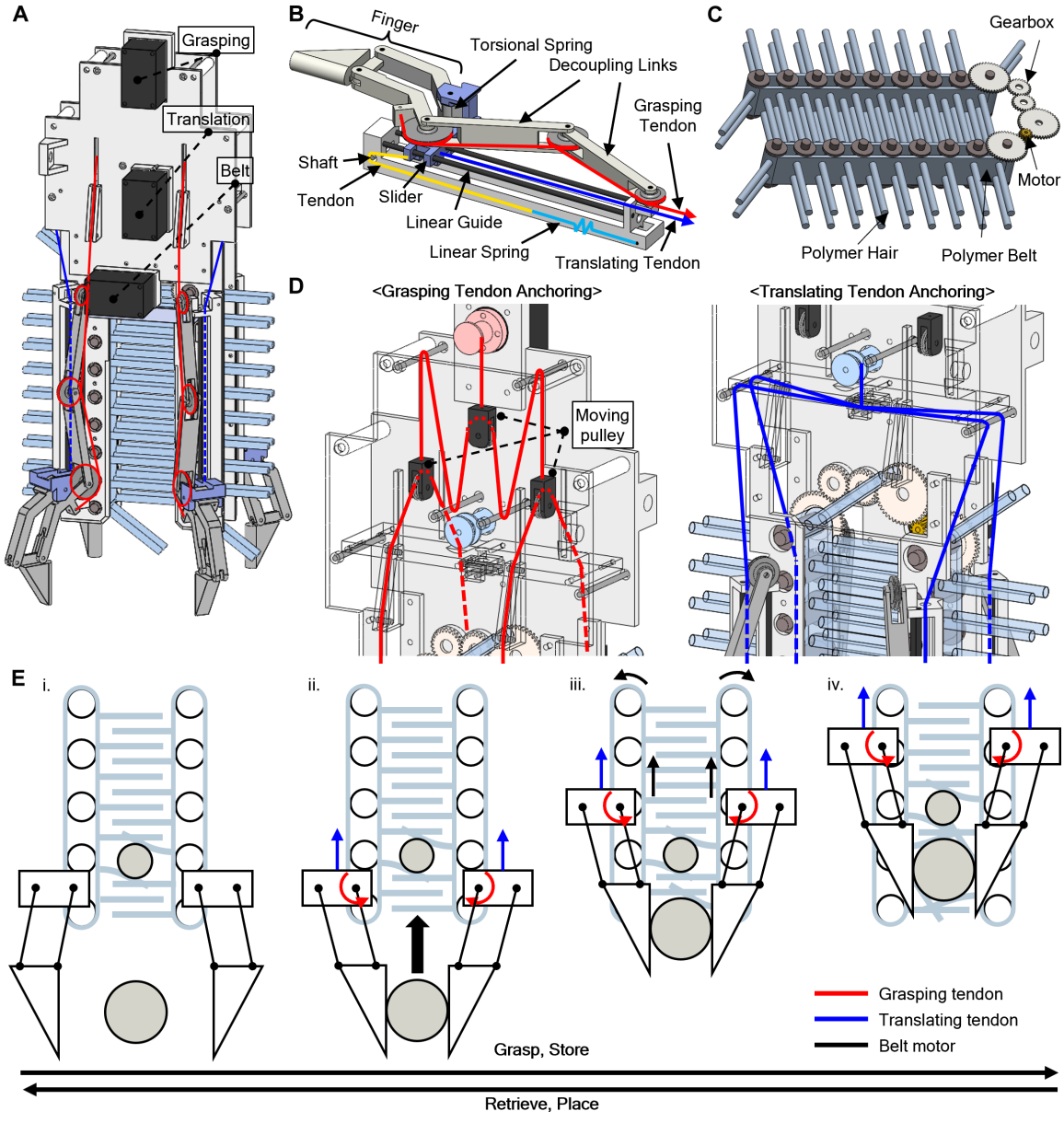

Fig. 2. Design and strategy of the multiobject gripper using translational movement of fingertips. (**A**) Overall design of the developed gripper. (**B**) Detailed design of a single finger. A finger made of a parallelogram linkage is placed on the slider, and a grasping tendon and a translating tendon are each connected with the finger and slider, creating rotation and translation of the finger. (**C**) Detailed design of the palm. The palm consists of two belts facing each other, and each belt has an array of elastomeric hairs on its surface. (**D**) Anchoring of the grasping tendon and the translating tendon. Four grasping tendons are underactuated using a moving pulley mechanism for adaptive grasping, and the four translating tendons are directly connected to the same pulley to ensure an equal translation distance for all four fingers. (**E**) Multiobject grasping strategy. The fingers grasp and transfer the object to the storage, and the palm inserts the object between the elastomeric hairs and stores it. By repeating the above procedure, the gripper can store multiple objects, transfer them at once, and retrieve and place the objects with the reverse process.

variations in the radii of the pulleys and lengths of links, we defined two nondimensional variables as shown in the equations below

$$\gamma = \frac{2r_2 - (r_1 + r_3)}{2r_3}, \quad \delta = \frac{l_2}{l_1} \tag{2}$$

Each tendon was assumed to be controlled through the position control of its corresponding motor.

Modeling and experiments on the finger's movement with changes in γ and δ were conducted (Fig. 3, F to I). The modeling results are illustrated in Fig. 3 (F and H) (see the "Coupled movements of the finger according to design variations in the decoupling links" section in Supplementary Methods for more details). The solid line represents the change in the finger's movements when only the grasping tendon is pulled, and the dotted line indicates the finger's movements when only the translating tendon is actuated.

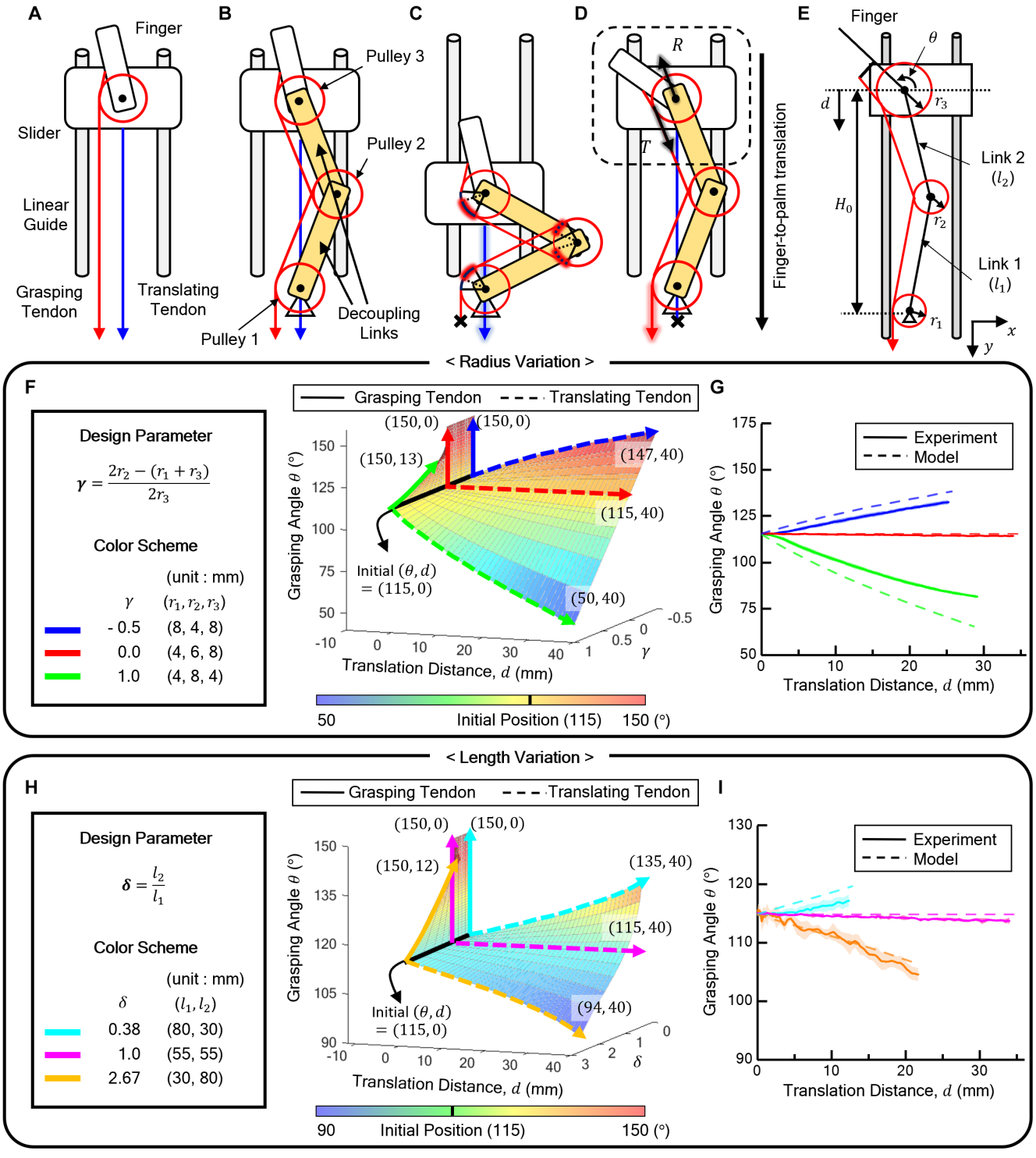

Fig. 3. Finger design for decoupling the grasping and translating movements. (**A**) Simple planar RP linkage example, where coupled tendon kinematics cause joint motions to be coupled. (**B**) Proposed RP linkage with decoupling links that prevent this coupling by decoupling the joint motions. (**C**) Decoupling links that maintain the length of the grasping tendon during finger translation. (**D**) Decoupling links that withstand pulling forces to prevent unintended finger translation. (**E**) Design parameters for studying the effective decoupling links. (**F**) Effect of pulley radius variations on fingertip motion. (**G**) Experimental fingertip motion while varying the radii of pulleys. (**H**) Effect of decoupling link length variations on fingertip motion. (**I**) Experimental fingertip motion varying the lengths of decoupling links. The mean ± 1 SD range of each experimental datum are indicated by the shaded regions [(G) and (I)]. Experiments for each design were conducted five times.

Specifically, when γ equaled 0 and δ equaled 1 (red lines in Fig. 3F and magenta lines in Fig. 3H), pulling the translating tendon only affected the translation distance, because pulling the grasping tendon exclusively altered the finger's grasping angle. Additionally, when γ was above 0 (green lines in Fig. 3F) or δ was greater than 1 (orange lines in Fig. 3H), actuating the translating tendon reduced the grasping angle and actuating the grasping tendon induced the translation of the finger. In contrast, when γ was below 0 (blue lines in Fig. 3F) or δ was less than 1 (cyan lines in Fig. 3H), actuating the translating tendon increased the grasping angle and actuating the grasping tendon did not lead to finger translation. The prevention of translation occurs because the translating tendon, which is directly connected to the slider, inhibits the finger translation in the negative y direction ($d < 0$).

To experimentally validate the derived design conditions (Eq. 1) of the decoupling linkage, the rotational and translational motions of fingers with various decoupling linkage designs were examined. To verify the decoupling of the two motions, the change in the grasping angle of the finger according to its translation distance was measured while pulling the translating tendon (fig. S2 and movie S1). The initial grasping angle of the finger was set to 115° by pulling the grasping tendon with a motor. Three markers were attached to the finger (fig. S2A), and the movements of the finger joints were recorded on video. Subsequently, the grasping angle (θ) and translation distance (d) of the finger were measured by tracking the markers through image analysis with MATLAB (fig. S2B). Five decoupling linkages with different design parameters were fabricated, and each was tested five times (table S1). The experimental results for the five designs are shown in Fig. 3 (G and I). The movement of the fingers with the five different designs closely matched the predictions of the analytic model. Detailed explanations of the experimental parameter selection and results can be found in the "Experimental parameter selection for validating the design conditions of decoupling links and experimental results" section in Supplementary Methods.

To successfully separate the finger's grasping and translation, the lengths of links 1 and 2 were determined to be 55 mm, and r_1, r_2, and r_3 were set to be 4, 6, and 8 mm, respectively, in accordance with Eq. 1. r_3 was set to be the largest to increase the gripper's grasping force. More details about grasping force can be found in fig. S3 and the "Maximum grasping force" section in Supplementary Methods. In addition, the resulting decoupled motions of the proposed fingers enabled the decoupled control of each motion through underactuation (Fig. 2D).

Conveyor palm design with hairy belt

A palm that can translate multiple objects between the storage and fingers and simultaneously store various objects was proposed. To simplify the object translating process, the proposed palm was designed to actively translate objects. This was because passive storage, such as a basket, may result in more difficult grasping issues when getting objects out of storage, as is often seen in bin-picking problems. Therefore, a belt system that can easily manipulate multiple objects with a single actuator was proposed as a storage. Objects were sandwiched between the two belts, stored in order, and delivered to the fingers in the reverse order of storage. Such active surfaces, like belts or rollers, have been widely used by conventional grippers to manipulate objects in desired directions while maintaining the grasp (*36*–*39*). In particular, robotic hands with fingers embedded within belt surfaces (*36*, *37*) demonstrated successful performance in various in-hand manipulation tasks. Although this flat belt design is powerful for in-hand manipulation of single objects, it faces challenges in simultaneously translating multiple stored objects. When storing multiple objects together, the flat elastic belt storage lacked the surface area in contact with small objects, resulting in unstable storage of differently sized objects (Fig. 4A, i) and storage failure of small objects (Fig. 4A, ii).

To stably store differently sized objects simultaneously between the two belts with a simple storing system, elastomeric hairs were embedded on the surfaces of the belts. Inserting objects between the hairy belts caused deformation in the hairs, generating a restoring force that stored the objects in place (Fig. 4A, iii). The storage of the palm was simplified by using this passive storing mechanism, which only used the rotation of the belts to translate and store objects. In addition, the hairy belt design allowed simultaneous storage of differently sized objects, because the hairs could ensure that the contact area for each object and the deformed hairs in contact with the object did not hinder the storage of other objects.

The maximum weight of the object that could be stored in the palm was analyzed. When an object was inserted into the palm, the object deformed the hairs substantially, and the hairs stochastically contacted each other, making analytical modeling difficult. Therefore, the maximum storable weight was experimentally measured and analyzed by finite element analysis (FEA). Because the storing force is generated by the passive deformation of the hairs, the hair design and object size are directly related to the maximum storable weight. Accordingly, we selected three parameters for validation: the radius of the hair (r), the distance between the hairs (b), and the size of the target (R) (Fig. 4B). The details regarding the corresponding parameter selection are available in Supplementary Methods and table S2 (see the "Parameter selection for validating the storing capability of the palm" section). In addition, the maximum storable weight of the palm varies depending on the direction of the gravitational force applied to the object. Therefore, both the storable weight along the y axis and the storable weight along the x axis were analyzed (Fig. 4B). Here, the storing force in each direction was defined as the maximum storable weight in that direction.

The mean storing force of an object along the y axis, its SD, and the FEA simulation results of each design are shown in Fig. 4 (C and D). The experimental setup is illustrated in fig. S4 (A to D), and the FEA simulation image is shown in fig. S4E. In Fig. 4, both C and D, the simulation results showed good agreement with the experimental results. Figure 4C shows the storing force along the y axis according to the changes in R and r when b was fixed at 20 mm. In both the experiment and simulation, as R increased, the storing force and the increment of storing force gradually increased. This was because the larger object induced more deformations in the contacting hairs, and the number of hairs in contact was higher compared with smaller objects. As r increased, the moment exerted on the hair by the object increased with the fourth power of r [eq. S43, equation 5.12 in (*40*)]. This implies that the force exerted by the hair on the object also increased with the fourth power of r. Furthermore, the curvature of the hair increased because the surfaces of the hair and the cylinder became closer. Therefore, the change in storing force according to the change in r was predicted to follow a slightly larger value than the fourth power of r, but the result was smaller. For example, the storing force of a cylinder with a radius of 17.5 mm was 35.3 gram-force (gf) (0.35 N) when r was 1.5 mm and 323.5 gf (3.17 N) when r was 3 mm. The difference between the two values

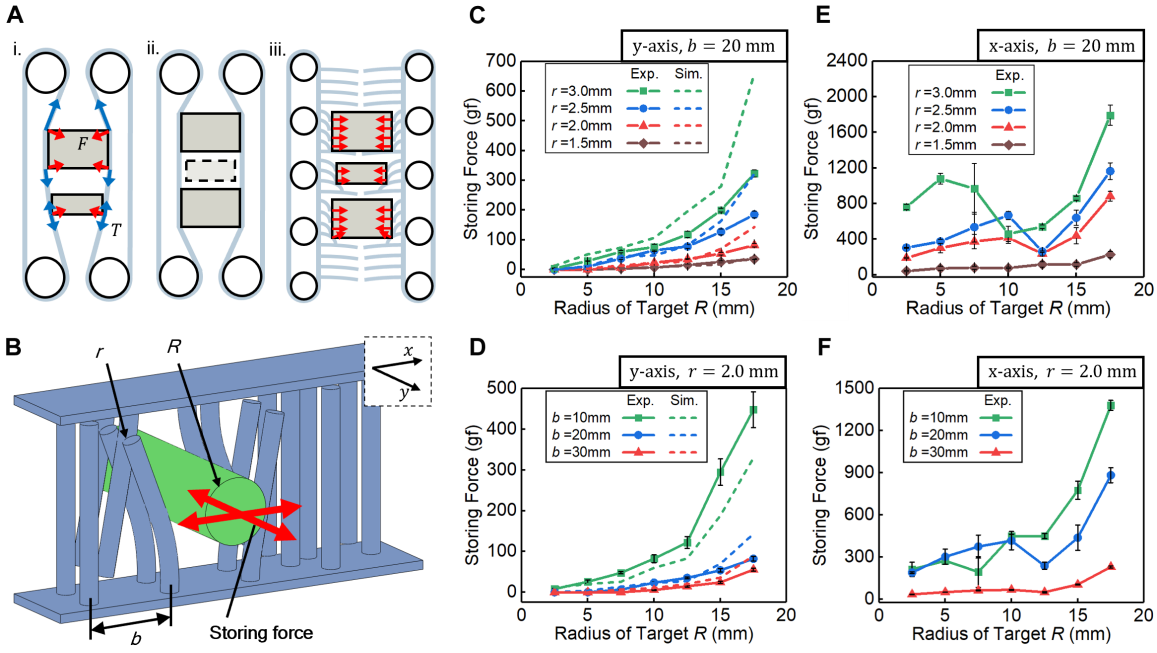

Fig. 4. Conveyor palm design for simultaneous translation and storage of multiple objects. (**A**) Comparison between hairless elastic belt storage (i and ii) and hairy elastic belt storage (iii). In the hairless elastic belt, the storage of an additional object results in additional deformation of the belt surfaces, (i) reducing the storing force of the stored objects and (ii) leading to storage failure of small objects. When the object is inserted into the hairy belt storage, (iii) the elastomeric hairs bend and independently push the object, allowing simultaneous storage of arbitrarily shaped objects. (**B**) Design parameters for investigating the storage force of the proposed conveyor palm. (**C** and **D**) Experimental and simulation results of the *y*-axis storing force in response to the radius of the target with storage designs of different (C) radii of hairs (b = 20 mm) and (D) distance between adjacent hairs (r = 2.0 mm). (**E** and **F**) Experimental results of the *x*-axis storing force in response to the radius of the target with storage designs of different (E) radii of hairs (b = 20 mm) and (F) distance between adjacent hairs (r = 2.0 mm). Experiments for each design were conducted five times, and error bars are used to represent the SD.

was ~9.2 times and did not exceed 16 times. This result is because the cylindrical-shaped hairs are unable to stack up perfectly, leading them to slide past each other. This sliding causes a change in the direction of hair bending, resulting in a decrease in the restoring force exerted by the hairs on the object in the normal direction.

Figure 4D shows the measured storing force along the y axis and the simulation result according to the change in R and b when r was fixed at 2 mm. Similar to the results in Fig. 4C, the increment of storing force gradually increased as R increased. Also, it is noteworthy that the change in b substantially shifted the storing force. This was because as b decreased, not only the distance between the object and the hair got closer but also the number of hairs touching the object increased. This also explains that the slope of the storing force increased substantially according to the change in r when b was small.

The mean storing force of an object along the x axis was also analyzed, and the results are shown in Fig. 4 (E and F). The experimental setup is described in fig. S5. For all palm designs, the x-axis storing force was smaller than the y-axis storing force (fig. S6). The x-axis storing force tended to increase, then decrease, and then increase again as the object's radius increased (Fig. 4, E and F). For example, the storing force of the palm design with r = 3.0 mm and b = 20 mm (green line in Fig. 4E) increased until R reached 5 mm, then decreased until R reached 10 mm, and then increased again. A detailed analysis of this phenomenon can be found in the "Detailed analysis of the trends in the storing force along the x-axis" section in Supplementary Methods and in fig. S7.

To better understand the simultaneous storing capability of multiple objects, the storing force of the cylindrical object was measured by changing the radius of the additional object (fig. S8). Given that the y-axis storing force was the weakest direction for the palm and the x-axis storing force was expected to have less variation, only the effect of additional objects on the y-axis storing force was analyzed. The distance between the two objects was set as 30 mm, and the radii of the additional objects were 7.5 and 17.5 mm (fig. S8A). The storing force was measured using the same setup used for the y-axis storing force measurement (fig. S8B). The storing force without an additional object was also measured for comparison. As a result, storing additional objects did not decrease the storing force but rather increased it (fig. S8C). This was because the additional object pushed the hairs between the two objects when it was stored, and the pushed hairs applied additional force to the previously stored object. Furthermore, as the size of the additional object increased, the hairs between the two objects became more compressed, resulting in an increase in the storing force. When the radius of the additional object was 7.5 and 17.5 mm, the storing force of the black cylinder increased by about 10% and 20%, respectively. In addition to the simultaneous storing capability, the scalability of the developed palm design was briefly studied (see the "Scalability of the conveyor palm" section in Supplementary Methods and fig. S9 for more details).

On the basis of the storing force experiments of various conveyor palm designs and theoretical analysis of scalability, design strategies can be developed to increase the storable weight and size limits of

the conveyor palm. First, to increase the storing force for objects with the same dimensions, design modifications can be considered, such as increasing the radii of the hairs (r) or decreasing the distance between hairs (b), as suggested by experimental results. Additionally, increasing the Young's modulus (E) of the material composing the hair or increasing the number of hairs in the width direction of the belt (y direction in Fig. 4B) is another viable method. Next, the size limit of storable objects is proportional to the gap between the two belts. Therefore, to store an object that is n times wider than the current size limit of the palm, the gap between the two belts needs to be increased by n times. According to the scalability analysis, if all design parameters are scaled up by a factor of n, the storing force will increase by a factor of n^2. These parameters include the gap between the belts, the radius (r) and length of the hairs, and the distance (b) between hairs. If the weight of the object exceeds the storable weight of the scaled-up palm, strategies to increase the storing force, as mentioned earlier, can be used to enhance the weight capacity. The storable weight of the scaled-up palm can be calculated by multiplying the current experimentally measured storing force by n^2.

Validation of the proposed gripper's translation process

To validate the developed gripper system, the robustness of the proposed gripper's manipulation skills (finger-to-palm translation and palm-to-finger translation) was studied through various experiments. First, the success rate and placement error of the proposed multiobject grasping sequence for various objects were studied (fig. S10). The experimental setup is described in fig. S10A. The proposed multiobject grasping sequence consists of grasping, storing, retrieving, and placing processes. Failure of this sequence was defined as cases where the finger or palm failed to properly grasp or store the object during the translation process between the finger and palm. Specifically, if the palm failed to store the object after finger-to-palm translation or if the finger failed to properly retrieve the object during palm-to-finger translation, the sequence was considered a failure. Failures were particularly frequent during the retrieval process, often because of the object being tilted or rotated in the palm (fig. S10B), preventing all four fingers from grasping it correctly.

The success rate and placement error were hypothesized to have different tendencies based on the curvature of the target objects' surfaces, so the target objects for the two experiments were chosen to be a cylinder and a cuboid (fig. S10C). However, because a cylinder can roll after being placed, making it difficult to accurately measure placement error, a cylinder with $^1/_{10}$ of its diameter sliced off was used. The diameter/width of the sliced cylinder/cuboid was set at intervals of 5 mm ranging from 5 to 35 mm, and each object was tested 20 times. The success rates for each object are shown in fig. S10 (D and E). For the sliced cylinder, the success rate increased until the diameter reached 20 mm, and all objects with diameters greater than 20 mm had 100% success rates. Sliced cylinders with smaller diameters often rolled between the adjacent hairs of the conveyor palm, resulting in lower success rates (fig. S10D). In contrast, the cuboid did not roll along the length of the hairs, resulting in a high success rate regardless of width (fig. S10E). The success rate was 90% when the width was 10 mm because, as shown in fig. S10B, the edges of the cuboid sometimes aligned with the intersections of the hairs, causing the cuboid to rotate and not be properly retrieved.

The placement errors for the sliced cylinders and cuboids of various sizes are shown in fig. S10 (F and G). The placement error of an object was defined by comparing the object's configuration before grasping and after placing, measuring the displacement of the center of mass (d_0) and the object's tilt angle (θ) (fig. S10A). For the sliced cylinder, both the displacement of the object center and the tilt angle decreased as the diameter increased. In the case of the cuboid, the tilt angle was nearly zero regardless of the object size, but the center displacement was around 2 to 4 mm irrespective of the object size.

To further investigate the limitations of the translation process for a grasped object, an analysis was also conducted on cases where the object was grasped off center from its center of mass (fig. S11) and where the translation direction of the object did not align with the direction of gravity (figs. S12 and S13). Detailed analyses for each case can be found in the "The success rate and placement error when a long object is grasped off-center" and "The effect of the object's weight, friction of the slider, and gripper tilt angle on palm-to-finger translation" sections in Supplementary Methods.

Demonstration of the proposed gripper's efficiency and pick-and-place abilities

To validate that the total pick-and-place process time and travel distance of the robot arm can be reduced through the proposed multiobject gripper, a logistics demonstration was conducted in a laboratory environment (Fig. 5A and movie S2). Using the proposed gripper, the time and travel distance required to place four objects in each of the two boxes were measured for both when the gripper moved a single object at a time and when it moved four objects simultaneously. As a result, when using single-object grasping, the travel distance of the manipulator's end effector was 29.5 m, and the overall process time was 1 min and 29 s, whereas when using multi-object grasping, the travel distance was 8.5 m, and the process time was 59 s (Fig. 5B). Therefore, the proposed gripper could reduce the travel distance by about 71% and the overall process time by about 34% in this demonstration. To validate the developed gripper's design, the theoretical minimum pick-and-place time was derived (see the "Comparison of manipulator travel length and process time between multi-object grasping and single-object grasping" section and fig. S14). The most efficient multiobject grasping could be achieved when the translation and storing process times were shorter than the manipulator's movement time, because these processes occur simultaneously with the manipulator's movement. The theoretical minimum pick-and-place process time, calculated by movie analysis of movie S2, was approximately 55 s, which was about 6.8% less than the actual demonstration time. This indicates that the translation and storing processes of the developed multiobject gripper are sufficiently short. To achieve a shorter process time, the use of faster and more powerful translating and storing motors could be considered.

An investigation of the efficiency of multiobject grasping compared with that of single-object grasping was also proposed (see the "Comparison of manipulator travel length and process time between multi-object grasping and single-object grasping" section in Supplementary Methods and fig. S14 for more details). The degree of shortening distance and time of multiobject grasping was larger when the distance between the objects got closer and the distance between the pick and place locations got farther. Consequently, the developed gripper is anticipated to be especially effective in

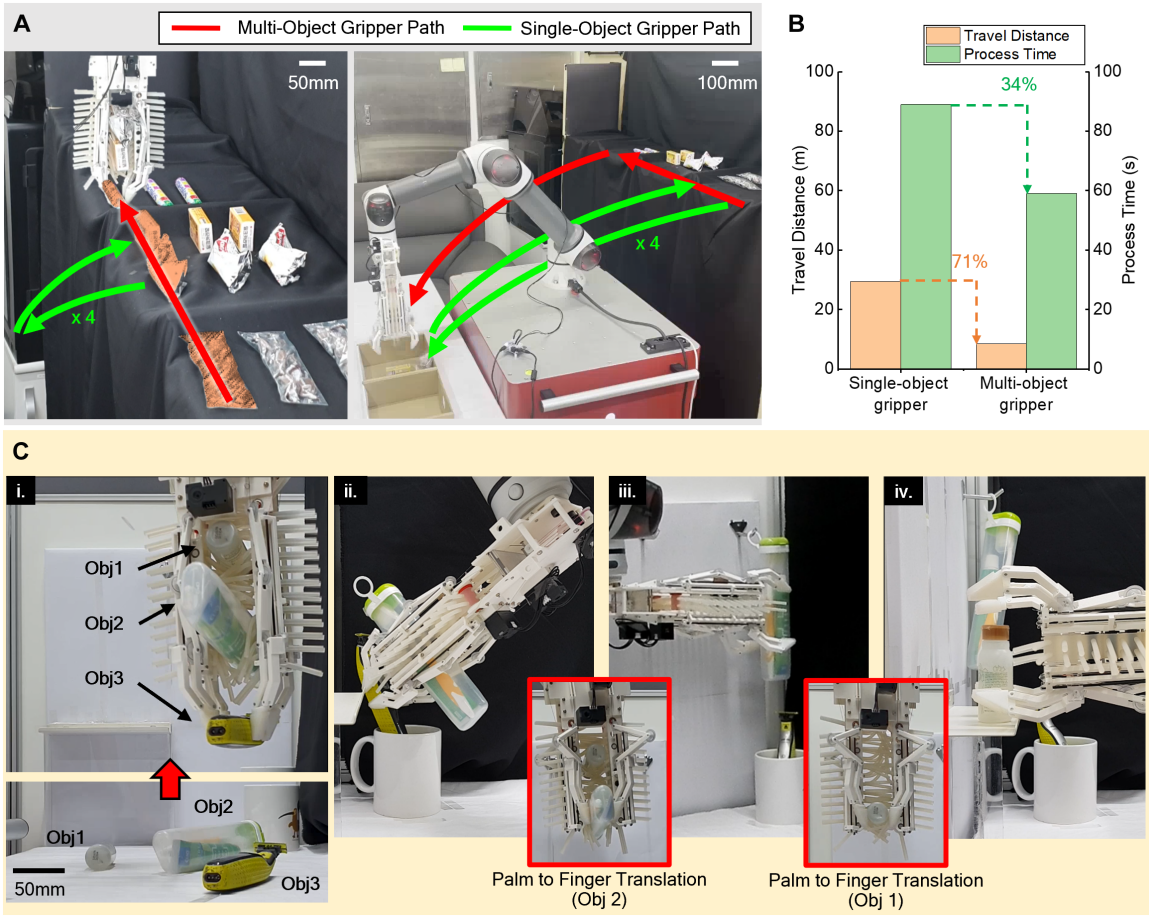

Fig. 5. Demonstration of the proposed multiobject gripper. (**A**) Logistic demonstration to compare the travel distance of the manipulator's end effector and the overall pick-and-place process time when using single-object grasping and multiobject grasping. (**B**) Comparison of travel distance and process time between single-object and multiobject grippers in a laboratory-scale logistics demonstration. The multiobject gripper can reduce the travel distance by about 71% and the overall process time by about 34% in this demonstration. (**C**) Domestic demonstration to verify the placing ability of the multiobject gripper. (i) The gripper can move multiple objects at once and place the (ii) razor, (iii) toothbrush set, and (iv) lotion in their desired places.

environments like logistics processes, where pick and place locations are distinctly separate. It is also expected to excel in scenarios such as households, where mobile manipulators are used to move between pick and place locations that are substantially distanced from each other. To further investigate the efficiency of the proposed multiobject grasping, a theoretical comparison with conventional multiobject grasping strategies was conducted (see the "Comparison of manipulator travel length and process time between various multi-object grasping strategies" section in Supplementary Methods for more details).

To verify that the proposed gripper can place the stored objects in their desired locations, we demonstrated a gripper tidying up a cluttered desk in a domestic environment (Fig. 5C and movie S3). The proposed gripper grasped a small lotion bottle and a travel toothbrush sequentially, translating them to the palm through finger-to-palm translation. After that, the gripper grasped a razor and transferred three objects simultaneously (Fig. 5C, i). Thereafter, the gripper placed the razor in a cup (Fig. 5C, ii) and retrieved the stored objects one by one to hang the toothbrush set on the wall (Fig. 5C, iii) and put the lotion bottle on the shelf (Fig. 5C, iv). The detailed specifications of the target objects are presented in table S3. Finally, as shown in fig. S15 and movie S4, the gripper successfully grasped, stored, retrieved, and placed 23 different types of objects. This result shows the gripper's grasping and retrieving abilities for various types of objects.

DISCUSSION

Here, a multiobject gripper for versatile pick-and-place operations in unstructured environments has been presented. The spatial separation of the finger and palm and their synergistic use, facilitated by the translational movements of the finger, allows the gripper to grasp and place objects relatively freely while moving multiple objects together. This expands the versatility of the multiobject gripper's pick-and-place capabilities. By repeating grasping and storing, the developed gripper can grasp distant objects sequentially and move them simultaneously. The gripper can also individually place objects in the desired configuration by retrieving the stored objects. A decoupling linkage and hairy belt storage design are proposed to simplify the additional translating and storing process of the developed multiobject grasping method. The laboratory-scale logistics demonstration has successfully shown

that the developed gripper could improve the time efficiency of the pick-and-place process. Moreover, through a demonstration of tidying up a desk with the developed gripper, the feasibility of placing objects one by one in desired orientations was verified.

Future work may focus on enhancing the gripper system through implementing a sensing system and modifying the finger design. The proposed gripper's multiobject grasping sequence can lead to changes in object orientation, so a sensing system to estimate orientation and a finger design to adjust orientation would improve operation. Bending or tactile sensors could detect object positions and orientations, facilitating more precise placement. Currently, although the sensing system detects a misalignment in the orientation of a retrieved object, reorienting objects for placement remains challenging. Modifying the finger design to increase its degrees of freedom could solve this issue. For instance, if the finger, slider, and decoupling linkage could rotate around the palm's longitudinal axis (y axis in Fig. 3E), the gripper could rotate an object while holding it. Alternatively, controlling each finger's translation with individual motors may allow the adjustment of an object while it is being grasped by the fingers. Additionally, adopting a finger design that passively switches between pinching and enveloping (*7*) would allow the fingers to deliver larger objects to the palm through enveloping rather than pinching.

The proposed multiobject grasping technique is expected to be suitable for unorganized environments and those with placement critical tasks. Therefore, we believe that our approach provides extended applications of multiobject grasping not only in logistics and domestic domains but also in unconstructed industrial settings like bin picking.

MATERIALS AND METHODS

Storage fabrication

The fabrication process of the hairy belts is shown in fig. S16. The proposed belts were molded with an elastomer (Dragon Skin 30, Smooth-On Inc.) using inner and outer molds (fig. S16A). To simplify the fabrication process, the belt and hairs were manufactured in one step through injection molding (fig. S16B). Air vents with a diameter of 0.5 mm were applied to prevent air traps at the tips of the hairs. After curing in an oven at 65°C for 1 hour, a long rectangular surface with embedded hairs was obtained (fig. S16C). After removing the thin cylinders made by the vents, an elastomeric adhesive (Sil-poxy, Smooth-On Inc.) was applied to attach both ends of the surface (fig. S16D).

Experiments

To validate the motion of the decoupling design, the grasping tendon was pulled with a motor (100:1 Micro Metal Gearmotor HPCB 6V, Pololu). The movement of five different decoupling linkages was recorded by a camera with 30 frames per second, and the positions of the three red markers of each frame were tracked through MATLAB (MathWorks). The MATLAB function "imfindcircle" was used to find the red markers, and through the positions of these three markers, the rotation angle and translation distance of the finger were calculated. Experiments were repeated five times.

The storing force along the y axis was measured by a tensile testing machine (INSTRON 5948 MicroTester). In the experiment measuring the storing force for a single object, to ensure repeatability in the process of inserting the object into the storage, the storage was divided in half and placed on both sides of the rail. Then, the target was placed between the storages, and stored by moving both storages to the center (fig. S4, B and C). Each stored target was pulled five times through a tensile testing machine at a speed of 30 mm/min, and the maximum pulling force was measured as the storing force (fig. S4D). The storing force was also analyzed using finite element simulation (fig. S4E).

Similarly, for the experiment on the simultaneous storing capability of two objects, the settings from the previous experiment (fig. S4, B and C) were used to ensure the reliability of the experimental setup. The storage was divided into three parts as shown in fig. S8A. The two objects were placed on both sides of the middle storage (highlighted in green), and the left and right storages (highlighted in orange) were moved to the center to store both objects. The black cylinder was pulled five times for each experiment at a speed of 30 mm/min through a tensile testing machine (INSTRON 5948 MicroTester), and the maximum pulling force was measured (fig. S8B).

The storing force along the x axis was measured by a load cell (KTOYO 333FDX) while pulling the objects using a linear motor (Actuonix P16-150-256-12-P) at a speed of 4.2 mm/s (fig. S5). For repeated experiments, a weight block was hung to apply force to insert the cylindrical object into the storage while rotating the belt. When calculating the storing force, the weight of the block was subtracted from the measurement obtained by the load cell. All experiments for each parameter were repeated five times.

In the experiment measuring the placement error of the multiobject grasping sequence, the configuration of the object before grasping and after placement was captured using a camera (ABKO APC900). Blue markers were placed at the center of mass of the object and at a point 30 mm along the length from that center. The position changes of the markers were measured using OpenCV. In the storing process of the multiobject grasping sequence, the distance at which each object was stored from the entrance of the storage was set to 30 mm.

Finite element analysis

FEA was conducted using the FEA software ABAQUS (ABAQUS 2023, Dassault systems). All simulation conditions were set to be identical to the experimental conditions. The belt surfaces opposite to the hair were set as a fixed boundary condition, and the gravitational force applied to the hair was also considered (fig. S4E, i). In addition, by dividing the simulation steps, the object was stored in the storage by pushing the hairs (fig. S4E, ii), and after the storing process was finished, the maximum pulling force was obtained by pulling the object (fig. S4E, iii). The objects were considered as a rigid body, and all contacts between the object and hairs and the hairs with each other were considered a general contact condition. Because dynamic motion occurs as the hair is pushed, the simulation was conducted through dynamic analysis. For the quasistatic assumption, both mass scaling and time period were set to 1, and the kinetic energy of the hair belt was less than 3% of the internal energy until the maximum storing force was measured.

Demonstration

All demonstrations were performed by attaching the gripper to a manipulator (RB5-850, Rainbow Robotics). In the time comparison test, the speed of the manipulator was 150 mm/s and the acceleration was 800 mm/s^2. In the third demonstration (movie S4), the

largest and heaviest target object was the NI myRio (National Instruments, size: 136 mm by 24 mm by 88 mm, weight: 195.07 g), the smallest object was a marble (size: 20 mm by 20 mm by 20 mm, weight: 12.00 g), and the lightest object was a vinyl package of chocolates (size: 10 mm by 25 mm by 70 mm, weight: 0.15 g).

Statistical analysis

All experiments, except for the success rate and placement error measurements, were repeated five times, and the mean values and SDs were calculated for each dataset. The SDs were represented as error bars. The success rate and placement error measurements were repeated 20 times per object, and their mean values and SDs were calculated, with SDs shown as error bars. Exceptionally, for the finger decoupling experiment (Fig. 3, G and I), because the x-axis data (translation distance) are continuous, the mean $\pm$ 1 SD range are represented as shaded regions. The demonstration comparing the efficiency of multiobject and single-object grasping was conducted once as a proof of concept.

Supplementary Materials

The PDF file includes:

Methods
Figs. S1 to S16
Tables S1 to S3
Legends for movies S1 to S4

Other Supplementary Material for this manuscript includes the following:

Movies S1 to S4

REFERENCES AND NOTES

1. Y. Sun, E. Amatova, T. Chen, Multi-object grasping—Types and taxonomy, in *Proceedings of the 2022 IEEE International Conference on Robotics and Automation* (IEEE, 2022), pp. 777–783.
2. C. E. Exner, in *Occupational Therapy for Children,* J. Case-Smith, Ed. (Elsevier Mosby, 2005), pp. 275–324.
3. K. Pont, M. Wallen, A. Bundy, Conceptualising a modified system for classification of in-hand manipulation. *Aust. Occup. Ther. J.* **56**, 2–15 (2009).
4. H. Yousef, M. Boukallel, K. Althoefer, Tactile sensing for dexterous in-hand manipulation in robotics—A review. *Sens. Actuators A Phys.* **167**, 171–187 (2011).
5. M. Visser, M. Nel, C. D. Plessis, S. Jacobs, A. Joubert, M. Muller, B. Smith, T. V. Heerden, R. V. Soest, In-hand manipulation (IHM) in children 6 and 7 years of age: A follow-up study. *S. Afr. J. Occup. Ther.* **46**, 52–58 (2016).
6. L. U. Odhner, L. P. Jentoft, M. R. Claffee, N. Corson, Y. Tenzer, R. R. Ma, M. Buehler, R. Kohout, R. D. Howe, A. M. Dollar, A compliant, underactuated hand for robust manipulation. *Int. J. Rob. Res.* **33**, 736–752 (2014).
7. M. Ciocarlie, F. M. Hicks, R. Holmberg, J. Hawke, M. Schlicht, J. Gee, S. Stanford, R. Bahadur, The velo gripper: A versatile single-actuator design for enveloping, parallel and fingertip grasps. *Int. J. Rob. Res.* **33**, 753–767 (2014).
8. M. G. Catalano, G. Grioli, E. Farnioli, A. Serio, C. Piazza, A. Bicchi, Adaptive synergies for the design and control of the Pisa/IIT SoftHand. *Int. J. Rob. Res.* **33**, 768–782 (2014).
9. R. Calandra, A. Owens, D. Jayaraman, J. Lin, W. Yuan, J. Malik, E. Adelson, S. Levine, More than a feeling: Learning to grasp and regrasp using vision and touch. *IEEE Robot. Autom. Lett.* **3**, 3300–3307 (2018).
10. W. Wan, K. Harada, Developing and comparing single-arm and dual-arm regrasp. *IEEE Robot. Autom. Lett.* **1**, 243–250 (2016).
11. Y. Zhao, J. Zhang, S. Zhang, P. Zhang, G. Dong, J. Wu, J. Zhang, Transporting dispersed cylindrical granules: An intelligent strategy inspired by an elephant trunk. *Adv. Intell. Syst.* **5**, 2300182 (2023).
12. V. P. Nguyen, W. T. Chow, Wiring-claw gripper for soft-stable picking up multiple objects. *IEEE Robot. Autom. Lett.* **8**, 3972–3979 (2023).
13. A. Shenoy, T. Chen, Y. Sun, Multi-object grasping—Efficient robotic picking and transferring policy for batch picking, in *Proceedings of the 2022 IEEE/RSJ International Conference on Intelligent Robots and Systems* (IEEE, 2022), pp. 2741–2747.
14. W. C. Agboh, J. Ichnowski, K. Goldberg, M. R. Dogar, Multi-object grasping in the plane. arXiv:2206.00229 [cs.RO] (2022).
15. Z. Ye, Y. Sun, Only pick once—Multi-object picking algorithms for picking exact number of objects efficiently. arXiv:2307.02662 [cs.RO] (2023).
16. S. Aeron, E. LLontop, A. Adler, W. C. Agboh, M. R. Dogar, K. Goldberg, Push-MOG: Efficient pushing to consolidate polygonal objects for multi-object grasping. arXiv:2306.14021 [cs.RO] (2023).
17. K. Srinivas, S. Ganti, R. Parikh, A. Ahmad, W. Agboh, M. Dogar, K. Goldberg, The busboy problem: Efficient tableware decluttering using consolidation and multi-object grasps. arXiv:2307.03882 [cs.RO] (2023).
18. W. C. Agboh, S. Sharma, K. Srinivas, M. Parulekar, G. Datta, T. Qiu, J. Ichnowski, E. Solowjow, M. Dogar, K. Goldberg, Learning to efficiently plan robust frictional multi-object grasps. arXiv:2210.07420 [cs.RO] (2022).
19. Y. Li, B. Liu, Y. Geng, P. Li, Y. Yang, Y. Zhu, T. Liu, S. Huang, Grasp multiple objects with one hand. arXiv:2310.15599 [cs.RO] (2023).
20. K. Yao, A. Billard, Exploiting kinematic redundancy for robotic grasping of multiple objects. *IEEE Trans. Robot.* **39**, 1982–2002 (2023).
21. Y. Chen, X. Gao, K. Yao, L. Niederhauser, Y. Bekiroglu, A. Billard, Differentiable robot neural distance function for adaptive grasp synthesis on a unified robotic arm-hand system. arXiv:2309.16085 [cs.RO] (2023).
22. P. Jiang, J. Oaki, Y. Ishihara, J. Ooga, Multiple-object grasping using a multiple-suction-cup vacuum gripper in cluttered scenes. arXiv:2304.10693 [cs.RO] (2023).
23. H. Li, X. Li, B. Wang, X. Shang, J. Yao, A fault-tolerant soft swallowing robot capable of grasping delicate structures underwater. *IEEE Robot. Autom. Lett.* **8**, 3302–3309 (2023).
24. S. E. Root, D. J. Preston, G. O. Feifke, H. Wallace, R. M. Alcoran, M. P. Nemitz, J. A. Tracz, G. M. Whitesides, Bio-inspired design of soft mechanisms using a toroidal hydrostat. *Cell Rep. Phys. Sci.* **2**, 100572 (2021).
25. C. Mucchiani, M. Yim, A novel underactuated end-effector for planar sequential grasping of multiple objects, in *Proceedings of the 2020 IEEE International Conference on Robotics and Automation* (IEEE, 2020), pp. 8935–8941.
26. J. R. Amend Jr., E. Brown, N. Rodenberg, H. M. Jaeger, H. Lipson, A positive pressure universal gripper based on the jamming of granular material. *IEEE Trans. Robot.* **28**, 341–350 (2012).
27. C. Wang, C. Linghu, S. Nie, C. Li, Q. Lei, X. Tao, Y. Zeng, Y. Du, S. Zhang, K. Yu, H. Jin, W. Chen, J. Song, Programmable and scalable transfer printing with high reliability and efficiency for flexible inorganic electronics. *Sci. Adv.* **6**, eabb2393 (2020).
28. A. M. Dollar, R. D. Howe, The highly adaptive SDM hand: Design and performance evaluation. *Int. J. Rob. Res.* **29**, 585–597 (2010).
29. D. Shah, A. Parmiggiani, Y.-J. Kim, Constant length tendon routing mechanism through axial joint, in *Proceedings of the 2020 IEEE/ASME International Conference on Advanced Intelligent Mechatronics* (IEEE, 2020), pp. 753–758.
30. R. Ozawa, H. Kobayashi, K. Hashirii, Analysis, classification, and design of tendon-driven mechanisms. *IEEE Trans. Robot.* **30**, 396–410 (2014).
31. S. Hirose, S. Ma, Coupled tendon-driven multi-joint manipulator, in *Proceedings of the 1991 IEEE International Conference on Robotics and Automation* (IEEE, 1991), pp. 1268–1275.
32. Y.-J. Kim, Y. Lee, J. Kim, J.-W. Lee, K.-M. Park, K.-S. Roh, J.-Y. Choi, RoboRay hand: A highly backdrivable robotic hand with sensorless contact force measurements, in *Proceedings of the 2014 IEEE International Conference on Robotics and Automation* (IEEE, 2014), pp. 6712–6718.
33. Z. Liang, B. Wang, Y. Song, T. Zhang, C. Xiang, Y. Guan, Design of a novel cable-driven 3-DOF series-parallel wrist module for humanoid arms, in *Proceedings of the 2021 IEEE International Conference on Mechatronics and Automation* (IEEE, 2021), pp. 709–714.
34. Y.-J. Kim, Anthropomorphic low-inertia high-stiffness manipulator for high-speed safe interaction. *IEEE Trans. Robot.* **33**, 1358–1374 (2017).
35. Q. Lu, N. Baron, A. B. Clark, N. Rojas, Systematic object-invariant in-hand manipulation via reconfigurable underactuation: Introducing the RUTH gripper. *Int. J. Rob. Res.* **40**, 1402–1418 (2021).
36. Y. Cai, S. Yuan, In-hand manipulation in power grasp: Design of an adaptive robot hand with active surfaces, in *Proceedings of the 2023 IEEE International Conference on Robotics and Automation* (IEEE, 2023), pp. 10296–10302.
37. V. Tincani, M. G. Catalano, E. Farnioli, M. Garabini, G. Grioli, G. Fantoni, A. Bicchi, Velvet fingers: A dexterous gripper with active surfaces, in *Proceedings of the 2012 IEEE/RSJ International Conference on Intelligent Robots and Systems* (IEEE, 2012), pp. 1257–1263.
38. S. Yuan, A. D. Epps, J. B. Nowak, J. K. Salisbury, Design of a roller-based dexterous hand for object grasping and within-hand manipulation, in *Proceedings of the 2020 IEEE International Conference on Robotics and Automation* (IEEE, 2020), pp. 8870–8876.
39. S. Yuan, L. Shao, C. L. Yako, A. Gruebele, J. K. Salisbury, Design and control of roller grasper v2 for in-hand manipulation, in *Proceedings of the 2020 IEEE/RSJ International Conference on Intelligent Robots and Systems* (IEEE, 2020), pp. 9151–9158.
40. J. M. Gere, B. J. Goodno, in *Mechanics of Materials* (Thomson Learning, ed. 6, 2004), pp. 309–314.

Acknowledgments: We thank the members of the Biorobotics Laboratory for the helpful discussions and feedback on the paper. **Funding:** This work was supported by a National Research Foundation of Korea (NRF) grant funded by the Korean government (MSIT) (RS-2023-00208052) (to K.-J.C.), providing 80% of the total funding, and by the Korea Institute of Science and Technology Institutional Programs under grant 2E33004 (to W.K.), providing the remaining 20%. **Author contributions:** J.E., W.K., and K.-J.C. conceptualized the research. J.E. designed and built the robots. J.E., S.Y.Y., C.P., and K.Y.L. designed the experiment, conducted experimental work, and performed demonstrations. J.E. conducted modeling and simulation. K.-J.C. supervised the project. J.E., S.Y.Y., W.K., and K.-J.C. wrote the paper. **Competing interests:** J.E., S.Y.Y., W.K., and K.-J.C. are included on a Korea patent (KR 10-2497956) that covers the multiobject grasping method using storage, which has been submitted by SNU R&DB Foundation. **Data and materials availability:** All data are available in the main text or the Supplementary Materials. The related data and code for this study have been deposited in Dyrad at https://doi.org/10.5061/dryad.44j0zpcqd.

Submitted 7 February 2024
Accepted 13 November 2024
Published 11 December 2024
10.1126/scirobotics.ado3939